Submitted: 20 May, 2022 Accepted: 10 June, 2022 Published: 15 April, 2023 DOI:10.22514/ejgo.2023.023

ORIGINAL RESEARCH

European Journal of Gynaecological Oncology

Identification of ferroptosis-related risk signature and correlation with the overall survival of ovarian cancer

Yibin Liu[1,†], Xin Xu[2,†], Jianlei Wu[3,†], Zhongkang Li[1], Ye Zhang[4], Xiaoxiao Zhang[4], Shike Shui[4], Hui Li[4], Tiantian Wang[4], Juan Zhai[4], Ruixia Guo[4,*], Yanpeng Tian[4,*]

[1]Department of Obstetrics and Gynecology, The Second Hospital of Hebei Medical University, 050000 Shijiazhuang, Hebei, China
[2]Department of Gynecological Endocrinology, Beijing Obstetrics and Gynecology Hospital, Capital Medical University, 100026 Beijing, China
[3]Department of Gynecological Oncology, Shandong Cancer Hospital and Institute, Shandong First Medical University and Shandong Academy of Medical Sciences, 250021 Jinan, Shandong, China
[4]Department of Obstetrics and Gynecology, The First Affiliated Hospital of Zhengzhou University, 450000 Zhengzhou, Henan, China

***Correspondence**
tianyanp2020@163.com
(Yanpeng Tian);
grxcdxzzu@163.com
(Ruixia Guo)

† These authors contributed equally.

Abstract

Ovarian cancer is a lethal female reproductive system malignancy. However, the physiological roles of ferroptosis in ovarian cancer remains unclear. In this study, biological information databases were screened to characterize and examine the differentially expressed ferroptosis-related genes between ovarian cancer and normal ovarian tissue, and to further investigate a novel risk signature for predicting the prognosis of ovarian cancer. Molecular and clinical data were retrieved from The Cancer Genome Atlas (TCGA) database. Based on these data, we identified differentially expressed ferroptosis-related genes, and construct a multigene risk signature by least absolute shrinkage and celection operator (LASSO) Cox regression to predict the prognosis of ovarian cancer. Univariate and multivariate Cox regression analysis were used to verify the prognostic value of the signature. We constructed a risk signature for ovarian cancer based on differentially expressed ferroptosis-related genes between normal ovarian samples and ovarian cancer samples. Referring to median risk score, patients were divided into high-risk group and low-risk group. We performed Cox regression analysis, principal component analysis (PCA), t-distributed stochastic neighbor embedding (t-SNE) analysis, Kaplan-Meier Survival analysis and receiver operating characteristic (ROC) curve to verify the accuracy of the predicted value of the risk signature. The overall survival rates in low-risk group was significantly higher than that in high-risk group. In addition, the area under the curve (AUC) of the ROC curve reached 0.684 at 1 year, 0.682 at 2 years and 0.661 at 3 years. Functional analysis indicated differentially expressed ferroptosis-related genes were enriched in immune-related cells. The ferroptosis-related genes signature could predict the prognosis of ovarian cancer. These genes might be potential therapeutic targets.

Keywords

Ovarian cancer; Ferroptosis; Risk signature; Prognosis; Overall survival

1. Introduction

Ovarian cancer is a lethal female reproductive system malignancy. Recent global epidemiological statistics showed that it was responsible for approximately 313,959 and 207,252 new ovarian cancer cases and related deaths in 2020, respectively [1, 2]. Although the 5-year survival rate of early-stage ovarian cancer may reach 90% [3, 4], most patients (~75%) are diagnosed with advanced-stage disease due to its indolent course. Therefore, the overall survival rate of ovarian cancer remains mediocre, at <30% [5]. Despite advances in cytoreductive surgery [6, 7], targeted therapies [8] and immunotherapies [9, 10] have significantly improved the survival rates of the patients over the past years, those with advanced-stage disease have lesser satisfactory responses and poor therapeutic outcomes. Thus, there is an urgency to clarify the carcinogenesis of ovarian cancer, discover novel targets, and develop more beneficial therapeutic strategies to improve the outcomes of ovarian cancer patients.

In recent years, ferroptosis, an iron-dependent cell death due to excessive lipid peroxidation, has received extensive attention [11]. It was reported in several biological processes and diseases. Recent findings indicate that ferroptosis potentially triggers cancer cell death, providing a novel therapeutic target for treatments. A previous study reported significantly greater iron levels in ovarian cancer tissues compared to normal adjacent tissues [12]. Hong *et al.* [8] found that ferroptosis was responsible for poly (ADP-ribose) polymerase inhibitors PARPi-mediated anti-tumor effects. Despite numerous research, the significance of ferroptosis and related genes in ovarian cancer remain ambiguous.

Here, we hypothesized that ferroptosis-related genes might be potential therapeutic targets in ovarian cancer. To confirm this hypothesis, we first identified differentially expressed ferroptosis-related genes between ovarian normal and cancer tissues, based on which we constructed a multigene risk

signature for patient stratification and prognostic estimation. Overall, our results confirmed ferroptosis-related genes as potential therapeutic targets in ovarian cancer.

2. Methods and materials

2.1 Resources and data retrieval

RNA sequencing data of normal (n = 88) and cancerous (n = 427) ovarian tissues were retrieved from The Cancer Genome Atlas (TCGA), strictly abiding by its respective guidelines (https://www.cancer.gov/tcga). In addition, we retrieved 60 ferroptosis-related genes based on a previous related study [13]. DESeq2, with $p < 0.05$ and a log Fold Change (logFC) ≥ 2, was used to identify differentially expressed ferroptosis-related genes between ovarian normal and cancer samples.

2.2 Identification of ferroptosis-related genes

Differentially expressed ferroptosis-related genes were determined based on the intersection between listed differentially expressed genes and ferroptosis-related genes. Then, the prognostic significance of these genes with ovarian cancer was evaluated. Univariate analyses identified 6 core genes significantly related to the patients' overall survival, their expression patterns were assessed using the R (version 3, R Foundation for Statistical Computing, Vienna, Austria) "heatmap" package, and correlations among the expressions of these core genes were analyzed using Pearson's correlation.

2.3 Constructing a Risk Prediction signature

The R "glmnet" package and least absolute shrinkage and selection operator (Lasso) Cox regression analyses were used for identifying the most promising candidate genes. Finally, 6 key genes were identified based on the relative coefficient *via* multiple regression analysis. The following formula was derived for risk score estimation: (0.376255766843764 × ALOX12) + (0.47921287370999 × CRYAB) + (−0.690609296701056 × SLC7A11) + (−0.897251166405754 × HSBP1) + (0.184628472638535 × STEAP3) + (0.511907671277879 × ACACA).

Based on the derived risk scores, the median value of the proposed signature was determined for stratifying ovarian cancer patients into a high- or low-risk group. The stratification accuracy was determined using principal component analysis (PCA). The R "tsne" package was used for t-distributed stochastic neighbor embedding (t-SNE) analysis, and risk score differences were illustrated using a risk score curve. Next, the sensitivity and specificity of the risk score were shown using an ROC curve. The Kaplan-Meier (KM) method was implemented to plot the survival curves of the two risk groups. The prognostic significance of the signature was assessed using univariate and multivariate Cox proportional hazard analyses to determine its association with overall survival and clinicopathological factors, including age, menopause status, stage and grade [13].

2.4 Immune infiltration levels evaluation

Gene Ontology (GO) and Kyoto Encyclopedia of Genes and Genomes (KEGG) analyses were conducted to better understand the biological functions and underlying pathways associated with the differentially expressed ferroptosis-related genes. Here, pathway and gene enrichment analyses were performed using Gene ontology (GO) and the Kyoto Encyclopedia of Genes and Genomes (KEGG). Enrichment levels and functions of immune cells in each ovarian cancer sample were quantified using singlesample gene set enrichment analysis (ssGSEA) in terms of ssGSEA scores.

2.5 Statement

This research strictly obeyed the guidelines of the TCGA database. The study protocols followed corresponding guidelines and regulations.

3. Results

3.1 Identification of differentially expressed ferroptosis-related genes

Assessment of the downloaded mRNA expression profile showed 17,892 genes differentially expressed between normal and cancerous ovarian tissues. Of them, 15,019 were down-regulated and 2873 were up-regulated (Fig. 1A). Subsequently, 60 ferroptosis-related genes identified from prior research were compared [13]. Then, 48 (46 up-regulated and 2 down-regulated) differentially expressed ferroptosis-related genes between normal and cancerous ovarian tissues were selected (Fig. 1B, Table 1). Univariate Cox analysis showed that *arachidonate 12-lipoxygenase* (*ALOX12*), *crystallin alpha-B Gene* (*CRYAB*), *solute carrier family 7 membrane 11* (*SLC7A11*), *heat shock factor binding protein 1* (*HSBP1*), *six-transmembrane epithelial antigen of the prostate 3* (*STEAP3*) and *Acetyl-CoA Carboxylase Alpha* (*ACACA*) were the 6 ferroptosis-related genes (core genes) associated with the prognosis of ovarian cancer patients. The corresponding heatmap is shown in Fig. 1C.

3.2 Kaplan-Meier Survival analysis of the 6 core genes

Kaplan-Meier survival analysis showed the 4 ferroptosis-related genes, *CRYAB, HSBP1, SLC7A11 and STEAP3*, were significantly related to ovarian cancer patients' survival, while *ACACA* and *ALOX12* were not associated with patient's survival (Fig. 2A–2F).

3.3 Risk signature Construction Using the TCGA Dataset

Fig. 3A illustrates the forest plot of the 6 core genes, which shows that *SLC7A11* and *HSBP1* had a significant inverse correlation with prognosis, while *ALOX12, CRYAB, STEAP3* and *ACACA* were positively correlated with prognosis. Correlation network analysis shows the relationship among these 6 core genes (Fig. 3B). LASSO analyses (Fig. 3C and 3D) showed that all 6 genes were the most promising candidate genes,

which were included in the risk score of the signature.

Next, the ovarian cancer patients were stratified into a high- or low-risk group using the calculated median risk score (Fig. 4A). Kaplan-Meier analysis indicated that the high-risk group had poorer prognoses compared with the low-risk group (Fig. 4B), with a 1-, 2- and 3-year ROC curve value of 0.684, 0.682 and 0.661, respectively (Fig. 4C). Further, the high-risk group had higher early mortality risks than the low-risk group (Fig. 4D). PCA and t-SNE analyses indicated that the signature could divide the patients into two directions (Fig. 4E and 4F).

3.4 Prognostic significance of the 6-gene signature

Univariate analyses showed that age (HR: 1.370, 95% CI: 1.057–1.774, $p = 0.017$) and risk score (HR: 2.789, 95% CI: 2.027–3.837, $p < 0.001$) were significant prognostic predictor for ovarian cancer. After controlling for other confounders, the risk score (HR: 2.811, 95% CI: 2.035–3.883, $p < 0.001$) was identified as an independent prognostic predictor for ovarian cancer patients' survival (Fig. 5A and 5B).

3.5 Functional analysis using GO and KEGG

GO analysis showed that the differentially expressed ferroptosis-related genes were enriched in the extracellular matrix, negatively regulated endopeptidase activity, and were cofactors for transport. KEGG analysis indicated that transcriptional misregulation in cancer was associated with ovarian cancer (Fig. 6A and 6B).

Next, ssGSEA was applied to evaluate the immune cell subpopulations and related pathways of the differentially expressed ferroptosis-related genes. The results showed significantly different immune cell subpopulations, such as macrophages, neutrophils, T-helper cells and regulatory T cells (TREG), between the low- and high-risk groups. However, the tumor immune responses of the two risk groups were not significantly different (Fig. 6C and 6D).

4. Discussion

The treatment of ovarian cancer is clinically challenging as most patients are identified when the cancer has already progressed to an advanced stage [1, 3, 5], resulting in a poor overall survival rate of <30% despite numerous achievements in surgery, chemotherapy, radiotherapy, targeted therapy and immunotherapy [5]. Thus, clarifying the pathogenesis of ovarian cancer and identifying novel targets are needed to improve its diagnosis and treatment. In this regard, increasing evidence suggests ferroptosis is associated with anti-cancer effects [14–18], but its impact in ovarian cancer remains unclear. In this present study, we identified ferroptosis-related genes associated with ovarian cancer, based on which we constructed a 6-gene risk signature, and the patients could be stratified into a low- or high-risk group. Further analyses showed that the signature was an independent factor for the overall survival of ovarian cancer patients. GO and KEGG analyses showed the differentially expressed ferroptosis-related genes were enriched in pathways associated with immune-related cells and transcriptional dysregulation in ovarian cancer.

In the past few decades, gynecologic and medical oncologists have constantly been working on identifying reliable prognostic biomarkers to improve ovarian cancer treatments and outcomes. However, changes in a single gene expression seem to have low predictive effects as various signaling pathways could regulate it. Constructing a multigene-signature prognostic model could strengthen prognostic accuracy and provide new insights for exploring novel targets for ovarian cancer. Our results identified 6 promising ferroptosis-related genes (*ALOX12, CRYAB, SLC7A11, HSBP1, STEAP3* and *ACACA*) and were included in the risk signature. They were previously reported to participate in physiological processes. For instance, *ACACA, SLC7A11* and *STEAP3* were reported to be involved in lipid metabolism, (anti) oxidant metabolism and iron homeostasis, respectively [13, 19, 20]. In addition, *ALOX12* is known as a lipoxygenase participating in lipid metabolism [21, 22]. These genes also demonstrated key roles in tumor initiation and progression.

SLC7A11 (Solute carrier family 7 member 11), commonly known as xCT, is involved in the Xc-system to mediate cystine uptake. A previous study indicated that blocking *SLC7A11* could strengthen ferroptosis by disrupting the redox state of cells [23]. A recent study showed that PARPi promoted ferroptosis in ovarian cancer cells by suppressing *SLC7A11*-mediated glutathione (GSH) synthesis [8]. Bioinformatic analyses also indicated *SLC7A11* as a promising therapeutic target in ovarian cancer [8, 22]. *ALOX12* was reportedly required for p53-mediated tumor inhibition by regulating ferroptosis [24], but in this present study, we found that it had no effects on the survival in our investigated cohort of patients. In addition, *ALOX12*-mediated tumor inhibition was shown to associate with *SCL7A11* [24], but the underlying mechanisms of *ALOX12* in ferroptosis remain to be further investigated. *ACACA* was reported to relate to poor prognoses in various tumors [25, 26], but similar to *ALOX12,* it showed no significant impact on ovarian cancer patients' survival. *STEAP3* was shown to be closely associated with iron homeostasis and inflammatory responses and reported to maintain tumor growth under hypoferric conditions [27, 28]. However, its roles in ovarian cancer are yet to be clarified. In our study, *STEAP3* was differentially expressed between ovarian normal and cancer tissues and was confirmed to be associated with poor prognosis, similar to *CRYAB* and *HSBP1*.

Our univariate analysis results identified both *ACACA* and *ALOX12* as potential factors affecting the prognosis of ovarian cancer patients. However, they were not independent prognostic factors by Kaplan-Meier survival analysis, which might be due to the small number of normal ovarian tissues or differences between the two analytic methods. Despite this, *ACACA* and *ALOX12* were still used in the signature due to their important roles in tumor initiation and progression.

There were some limitations in this present study, such as the relatively limited number of normal ovarian samples and lack of basic research experiments and validation using clinical samples. Further, the underlying mechanism *via* which the ferroptosis-related genes affect ovarian cancer was not investigated. Thus, further studies are required to clarify these limitations.

TABLE 1. Differentially expressed ferroptosis-related genes.

Genes	logFC	*p* Value	Regulated
AKR1C1	−2.42580288	7.43×10^{-32}	Down-Regulated
AKR1C2	−2.01519516	2.39×10^{-18}	Down-Regulated
ALOX15	1.04351906	1.66×10^{-5}	Up-Regulated
PTGS2	1.04475798	3.29×10^{-7}	Up-Regulated
ACACA	1.12459081	1.22×10^{-24}	Up-Regulated
EMC2	1.16562385	6.18×10^{-28}	Up-Regulated
GCLC	1.17078069	2.76×10^{-25}	Up-Regulated
NFS1	1.18425411	1.94×10^{-35}	Up-Regulated
HMGCR	1.41135598	3.98×10^{-34}	Up-Regulated
CRYAB	1.41814040	1.78×10^{-10}	Up-Regulated
SAT1	1.46298201	3.51×10^{-22}	Up-Regulated
G6PD	1.51422835	7.82×10^{-43}	Up-Regulated
ALOX12	1.55350360	9.30×10^{-18}	Up-Regulated
RPL8	1.61855524	1.87×10^{-27}	Up-Regulated
FDFT1	1.62085750	1.72×10^{-37}	Up-Regulated
ACSL4	1.66629091	1.50×10^{-38}	Up-Regulated
ACSL3	1.68111945	6.44×10^{-55}	Up-Regulated
CARS	1.74204665	9.55×10^{-57}	Up-Regulated
PHKG2	1.78079986	1.94×10^{-65}	Up-Regulated
NOX1	1.79137988	5.06×10^{-34}	Up-Regulated
ABCC1	1.84005167	1.21×10^{-51}	Up-Regulated
GLS2	1.87964738	2.39×10^{-33}	Up-Regulated
HSBP1	1.90562392	7.12×10^{-58}	Up-Regulated
SLC1A5	1.97452029	3.15×10^{-52}	Up-Regulated
FADS2	2.00316247	4.29×10^{-25}	Up-Regulated
CS	2.04310313	3.90×10^{-74}	Up-Regulated
GOT1	2.06288473	4.09×10^{-63}	Up-Regulated
NCOA4	2.19204630	7.08×10^{-77}	Up-Regulated
CISD1	2.22885733	4.38×10^{-78}	Up-Regulated
PGD	2.26243942	1.38×10^{-74}	Up-Regulated
KEAP1	2.30249585	4.25×10^{-79}	Up-Regulated
TP53	2.31382078	3.89×10^{-35}	Up-Regulated
FANCD2	2.33287111	9.00×10^{-80}	Up-Regulated
LPCAT3	2.48498651	6.48×10^{-75}	Up-Regulated
GPX4	2.48603437	1.88×10^{-72}	Up-Regulated
GSS	2.49657866	5.98×10^{-99}	Up-Regulated
STEAP3	2.54364510	1.60×10^{-50}	Up-Regulated
CD44	2.60156542	6.14×10^{-52}	Up-Regulated
FTH1	2.63853773	7.97×10^{-57}	Up-Regulated
GCLM	2.82223740	2.96×10^{-98}	Up-Regulated
ATP5MC3	2.88049019	1.71×10^{-92}	Up-Regulated
SQLE	2.89059744	2.25×10^{-78}	Up-Regulated
HSPB1	3.08281700	2.47×10^{-66}	Up-Regulated
ALOX5	3.37107141	4.08×10^{-62}	Up-Regulated
SLC7A11	3.93761461	9.31×10^{-70}	Up-Regulated
NQO1	4.15476949	3.77×10^{-88}	Up-Regulated
CHAC1	5.01736600	8.94×10^{-124}	Up-Regulated
MT1G	7.17871586	5.59×10^{-93}	Up-Regulated

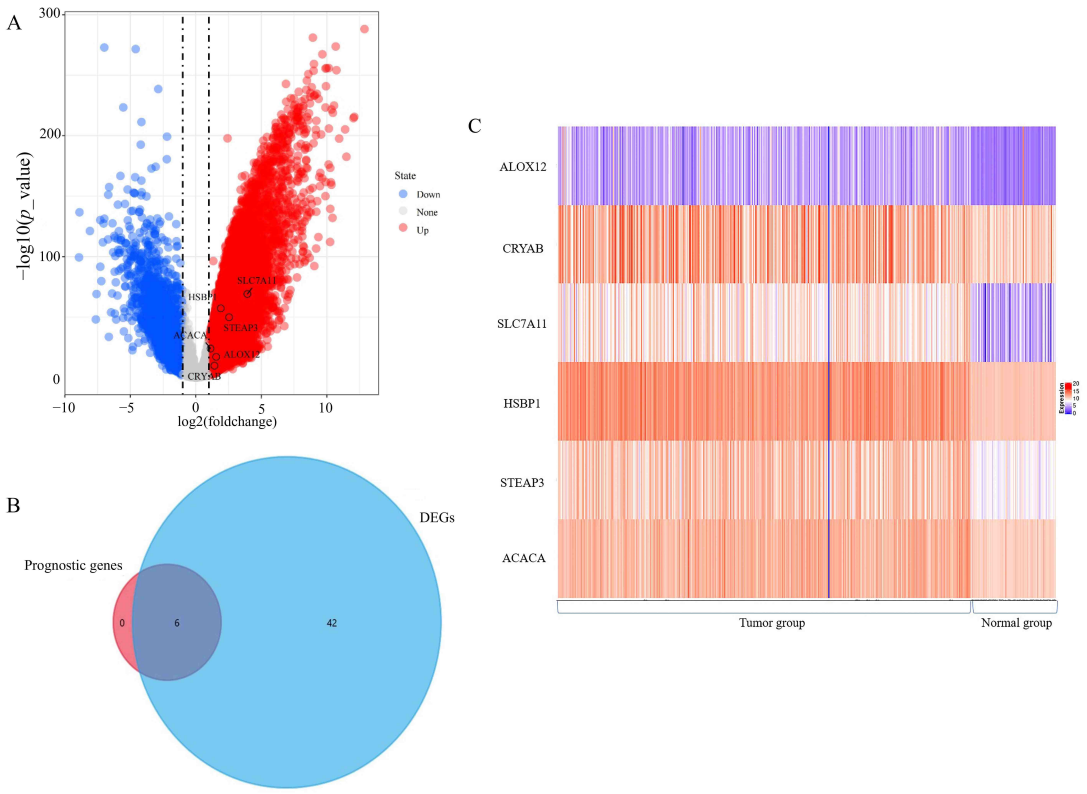

FIGURE 1. Identification of differentially expressed genes and association of ferroptosis-related genes with prognosis. (A) Volcano plots of differentially expressed genes. (B) Venn diagram of differentially expressed ferroptosis-related genes. (C) Heat map of the 6 differentially expressed ferroptosis-related genes associated with ovarian cancer prognosis.

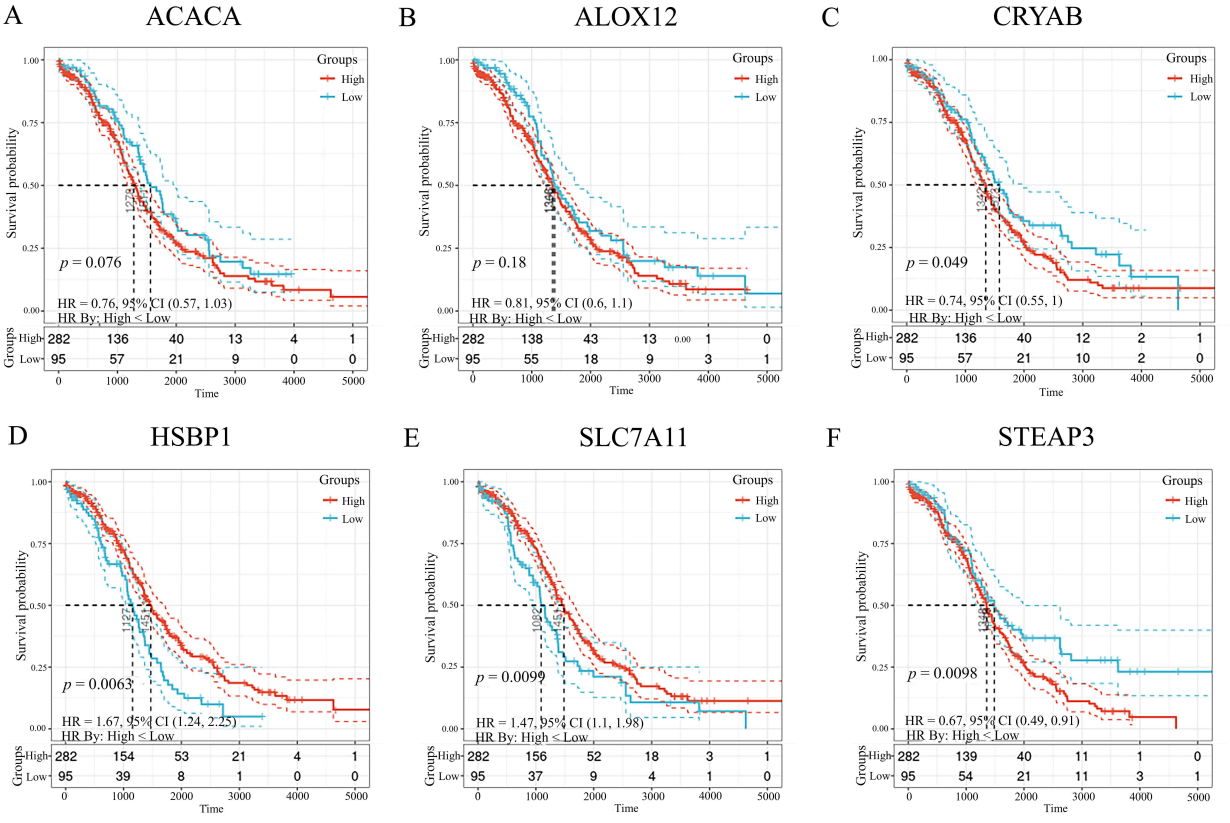

FIGURE 2. Kaplan-Meier survival analysis of ferroptosis-related genes. (A) *ACACA*. (B) *ALOX12*. (C) *CRYAB*. (D) *HSBP*. (E) *SLC7A11*. (F) *STEAP3*. Blue lines represent the low-risk group, and red lines represent the high-risk group.

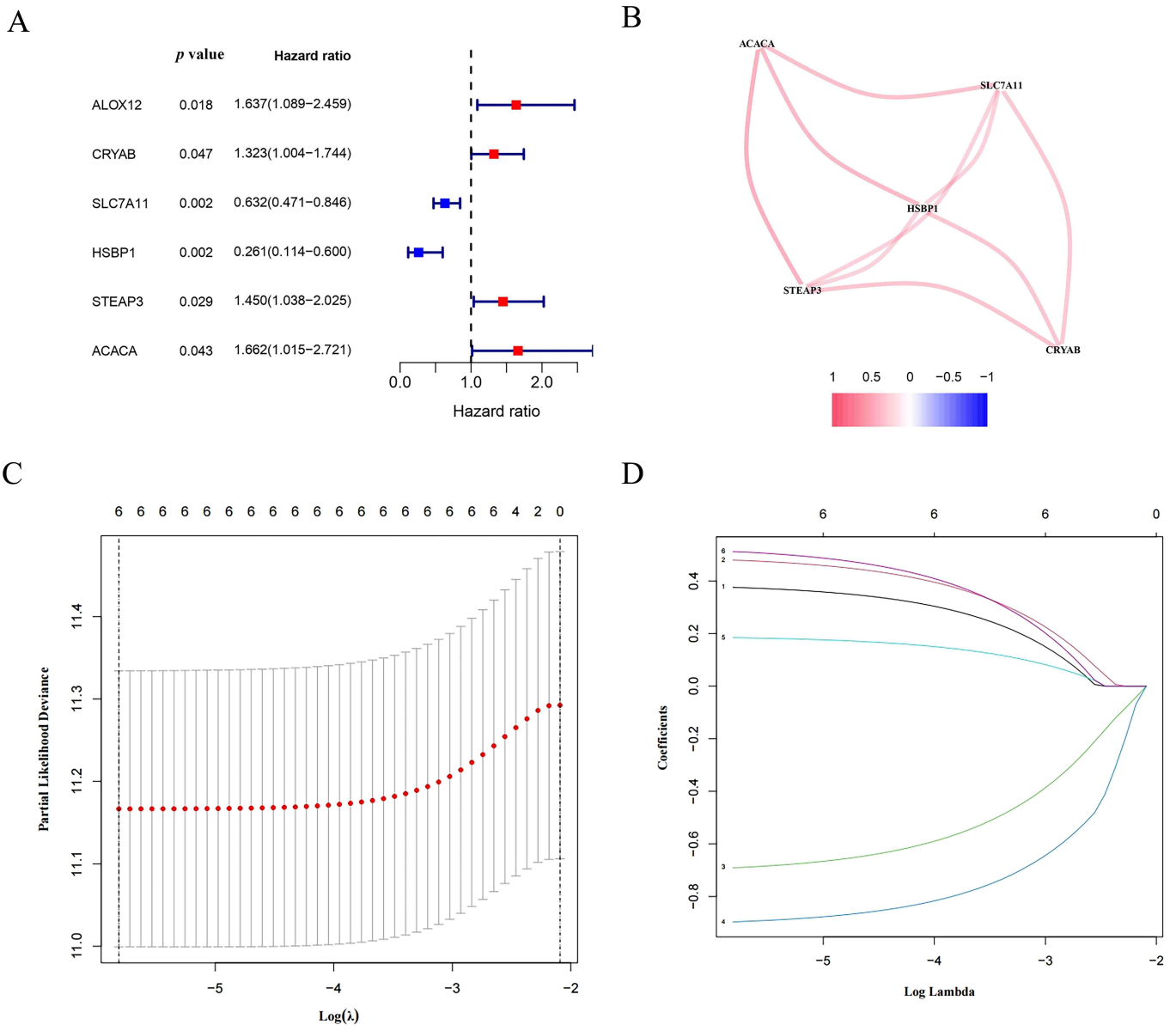

FIGURE 3. Correlation analysis of differentially expressed genes in ovarian cancer and construction of the LASSO regression model. (A) Univariate Cox regression analysis on the 6 differentially expressed ferroptosis-related genes. (B) Correlation analysis among these 6genes. (C) LASSO deviance profiles. (D) LASSO coefficient profiles.

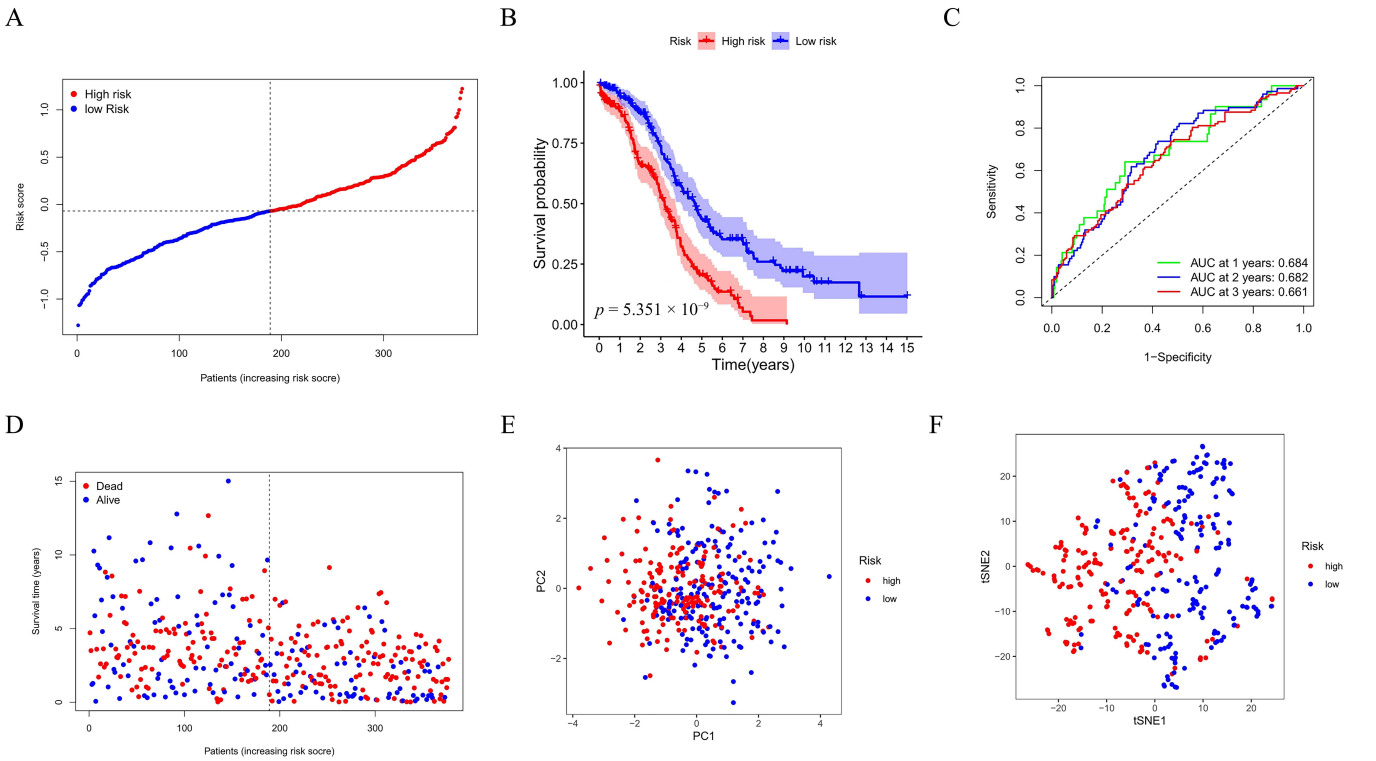

FIGURE 4. Construction of risk signature for ovarian cancer patients. (A) Risk score for ovarian cancer (B) Survival differences between the two risk groups evaluated using the Kaplan-Meier method. (C) ROC curves demonstrating the predictive efficiency of the signature. (D) Survival status for each patient. (E) PCA plot of ovarian cancer patients. (F) t-SNE analysis for ovarian cancer patients.

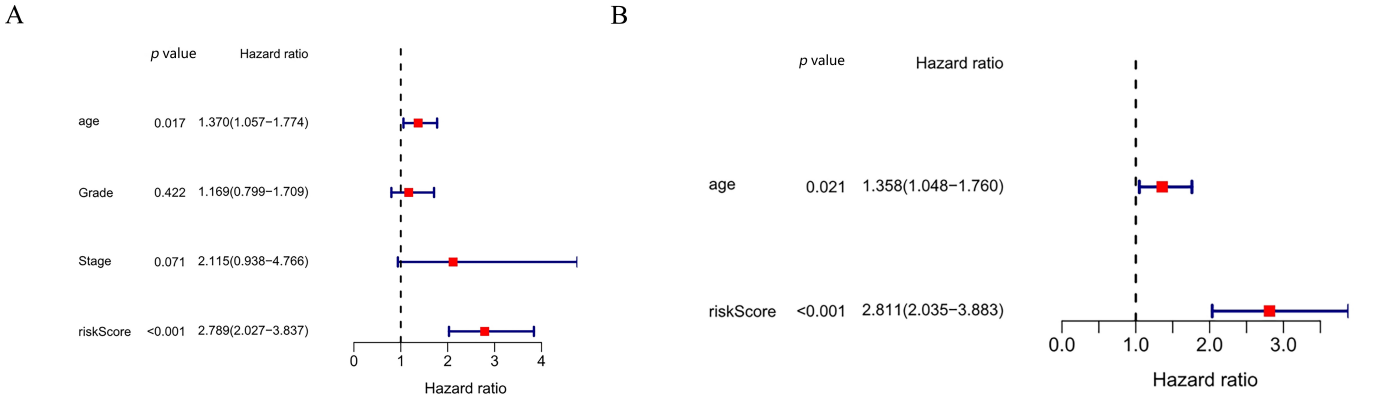

FIGURE 5. Univariate and multivariate Cox regression analysis for overall survival of ovarian cancer patients. (A) Univariate Cox regression analysis. (B) Multivariate Cox regression analysis.

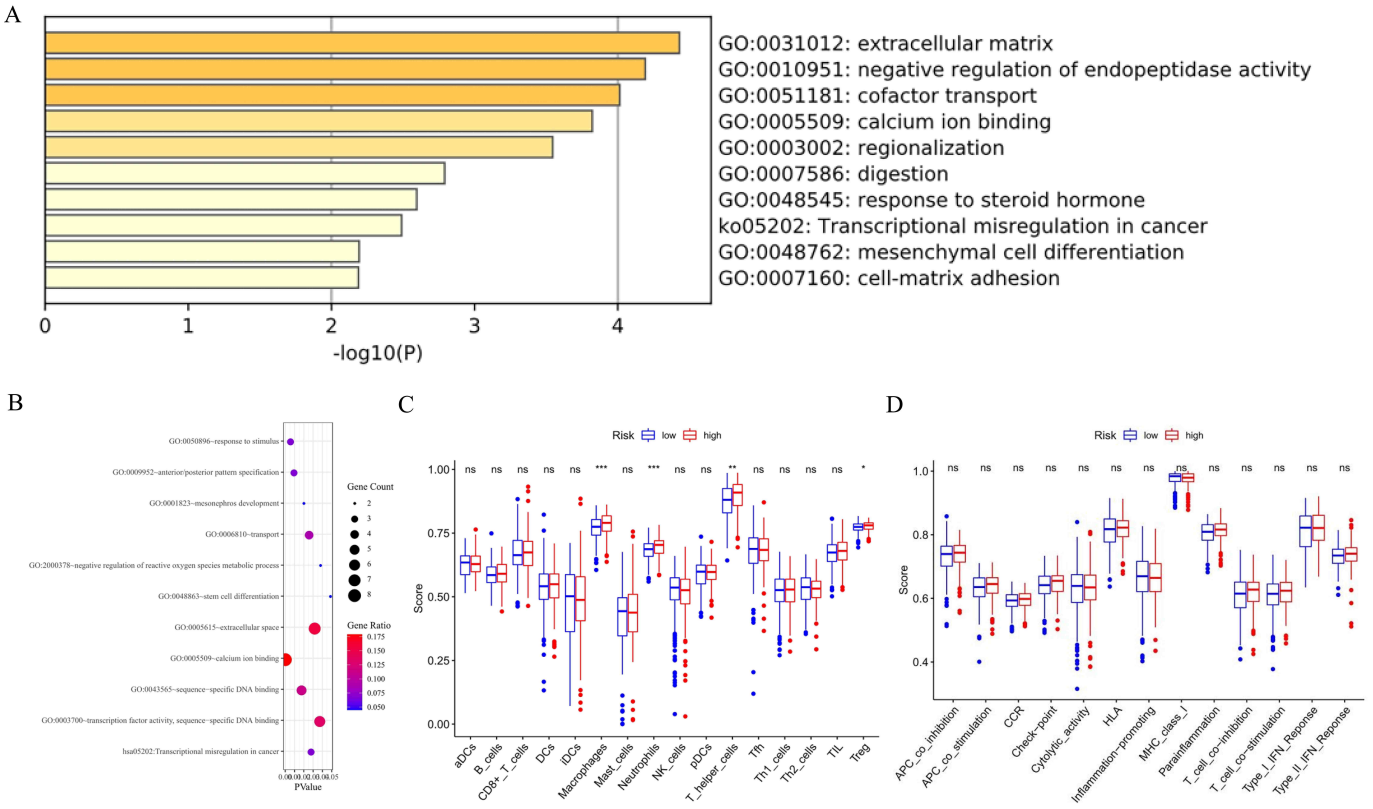

FIGURE 6. Functional analysis based on the differentially expressed ferroptosis-related genes between the two-risk groups. (A) Barplot graph for GO enrichment. (B) Bubble graph for GO enrichment. (C) Comparison of immune cell infiltration between the two groups. (D) Comparison of the immune functions between the two groups.

5. Conclusions

ALOX12, CRYAB, SLC7A11, HSBP1, STEAP3 and *ACACA* were identified as differentially expressed ferroptosis-related genes associated with the survival of ovarian cancer patients. They were to construct a 6-gene signature which showed promising efficacy in risk stratification and prognostic prediction. Altogether, our findings shed new insights into novel and potential targets for ovarian cancer.

AVAILABILITY OF DATA AND MATERIALS

The data presented in this study are available on reasonable request from the corresponding author.

AUTHOR CONTRIBUTIONS

RXG, YPT—Conception and design; YBL, XX, JLW—Provision of study materials or patients; ZKL, YZ—Collection and assembly of data; XXZ, SKS, JZ—Data analysis and interpretation; All authors—Manuscript writing and Final approval of manuscript.

ETHICS APPROVAL AND CONSENT TO PARTICIPATE

Not applicable.

ACKNOWLEDGMENT

The authors sincerely acknowledge the publicly available ImmPort database (https://immport.niaid.nih.gov) and TCGA (https://portal.gdc.cancer.gov/) database.

FUNDING

This research received no external funding.

CONFLICT OF INTEREST

The authors declare no conflict of interest.

REFERENCES

[1] Sung H, Ferlay J, Siegel RL, Laversanne M, Soerjomataram I, Jemal A, *et al*. Global cancer statistics 2020: GLOBOCAN estimates of incidence and mortality worldwide for 36 cancers in 185 countries. CA: A Cancer Journal for Clinicians. 2021; 71: 209–249.

[2] Feng P, Ge Z, Guo Z, Lin L, Yu Q. A comprehensive analysis of the downregulation of miRNA-1827 and its prognostic significance by targeting SPTBN2 and BCL2L1 in ovarian cancer. Frontiers in Molecular Biosciences. 2021; 8: 687576.

[3] Lu KH. Screening for ovarian cancer in asymptomatic women. JAMA. 2018; 319: 557.

[4] Choi P, Bahrampour A, Ng S, Liu SK, Qiu W, Xie F, *et al*. Characterization of miR-200 family members as blood biomarkers for human and laying hen ovarian cancer. Scientific Reports. 2020; 10: 20071.

[5] Liu R, Zeng Y, Zhou C, Wang Y, Li X, Liu Z, *et al*. Long noncoding

RNA expression signature to predict platinum-based chemotherapeutic sensitivity of ovarian cancer patients. Scientific Reports. 2017; 7: 18.

[6] Feng Z, Wen H, Jiang Z, Liu S, Ju X, Chen X, *et al*. A triage strategy in advanced ovarian cancer management based on multiple predictive models for R0 resection: a prospective cohort study. Journal of Gynecologic Oncology. 2018; 29: e65.

[7] Laios A, Gryparis A, DeJong D, Hutson R, Theophilou G, Leach C. Predicting complete cytoreduction for advanced ovarian cancer patients using nearest-neighbor models. Journal of Ovarian Research. 2020; 13: 117.

[8] Hong T, Lei G, Chen X, Li H, Zhang X, Wu N, *et al*. PARP inhibition promotes ferroptosis *via* repressing SLC7a11 and synergizes with ferroptosis inducers in BRCA-proficient ovarian cancer. Redox Biology. 2021; 42: 101928.

[9] Wan C, Keany MP, Dong H, Al-Alem LF, Pandya UM, Lazo S, *et al*. Enhanced efficacy of simultaneous PD-1 and PD-L1 immune checkpoint blockade in high-grade serous ovarian cancer. Cancer Research. 2021; 81: 158–173.

[10] Farkkila A, Gulhan DC, Casado J, Jacobson CA, Nguyen H, Kochupurakkal B, *et al*. Immunogenomic profiling determines responses to combined PARP and PD-1 inhibition in ovarian cancer. Nature Communications. 2020; 11: 1459.

[11] Hirschhorn T, Stockwell BR. The development of the concept of ferroptosis. Free Radical Biology and Medicine. 2019; 133: 130–143.

[12] Basuli D, Tesfay L, Deng Z, Paul B, Yamamoto Y, Ning G, *et al*. Iron addiction: a novel therapeutic target in ovarian cancer. Oncogene. 2017; 36: 4089–4099.

[13] Liang J, Wang D, Lin H, Chen X, Yang H, Zheng Y, *et al*. A novel ferroptosis-related gene signature for overall survival prediction in patients with hepatocellular carcinoma. International Journal of Biological Sciences. 2020; 16: 2430–2441.

[14] Jiang L, Kon N, Li T, Wang S, Su T, Hibshoosh H, *et al*. Ferroptosis as a p53-mediated activity during tumour suppression. Nature. 2015; 520: 57–62.

[15] Lang X, Green MD, Wang W, Yu J, Choi JE, Jiang L, *et al*. Radiotherapy and immunotherapy promote tumoral lipid oxidation and ferroptosis *via* synergistic repression of SLC7a11. Cancer Discovery. 2019; 9: 1673–1685.

[16] Friedmann Angeli JP, Krysko DV, Conrad M. Ferroptosis at the crossroads of cancer-acquired drug resistance and immune evasion. Nature Reviews Cancer. 2019; 19: 405–414.

[17] You Y, Fan Q, Huang J, Wu Y, Lin H, Zhang Q. Ferroptosis-related gene signature promotes ovarian cancer by influencing immune infiltration and invasion. Journal of Oncology. 2021; 2021: 1–16.

[18] Yang L, Tian S, Chen Y, Miao C, Zhao Y, Wang R, *et al*. Ferroptosis-related gene model to predict overall survival of ovarian carcinoma. Journal of Oncology. 2021; 2021: 1–14.

[19] Hassannia B, Vandenabeele P, Vanden Berghe T. Targeting ferroptosis to iron out cancer. Cancer Cell. 2019; 35: 830–849.

[20] Yimit A, Adebali O, Sancar A, Jiang Y. Differential damage and repair of DNA-adducts induced by anti-cancer drug cisplatin across mouse organs. Nature Communications. 2019; 10: 309.

[21] Zheng Z, Li Y, Jin G, Huang T, Zou M, Duan S. The biological role of arachidonic acid 12-lipoxygenase (ALOX12) in various human diseases. Biomedicine & Pharmacotherapy. 2020; 129: 110354.

[22] Ye Y, Dai Q, Li S, He J, Qi H. A novel defined risk signature of the ferroptosis-related genes for predicting the prognosis of ovarian cancer. Frontiers in Molecular Biosciences. 2021; 8: 645845.

[23] Goji T, Takahara K, Negishi M, Katoh H. Cystine uptake through the cystine/glutamate antiporter xCT triggers glioblastoma cell death under glucose deprivation. Journal of Biological Chemistry. 2017; 292: 19721–19732.

[24] Chu B, Kon N, Chen D, Li T, Liu T, Jiang L, *et al*. ALOX12 is required for p53-mediated tumour suppression through a distinct ferroptosis pathway. Nature Cell Biology. 2019; 21: 579–591.

[25] Chajes V, Cambot M, Moreau K, Lenoir GM, Joulin V. Acetyl-CoA carboxylase alpha is essential to breast cancer cell survival. Cancer Research. 2006; 66: 5287–5294.

[26] Fang W, Cui H, Yu D, Chen Y, Wang J, Yu G. Increased expression of phospho-acetyl-CoA carboxylase protein is an independent prognostic factor for human gastric cancer without lymph node metastasis. Medical Oncology. 2014; 31: 15.

[27] Liang C, Zhang X, Yang M, Dong X. Recent progress in ferroptosis inducers for cancer therapy. Advanced Materials. 2019; 31: 1904197.

[28] Yu Z, He H, Chen Y, Ji Q, Sun M. A novel ferroptosis related gene signature is associated with prognosis in patients with ovarian serous cystadenocarcinoma. Scientific Reports. 2021; 11: 11486.

How to cite this article: Yibin Liu, Xin Xu, Jianlei Wu, Zhongkang Li, Ye Zhang, Xiaoxiao Zhang, *et al*. Identification of ferroptosis-related risk signature and correlation with the overall survival of ovarian cancer. European Journal of Gynaecological Oncology. 2023; 44(2): 58-66. doi: 10.22514/ejgo.2023.023.